Vertical correlations and anticorrelations in multisheet arrays of two-dimensional islands

V. A. Shchukin* and D. Bimberg
Technische Universität Berlin, Hardenbergstraße 36, Berlin D-10623, Germany

V. G. Malyshkin and N. N. Ledentsov
A. F. Ioffe Physical Technical Institute, St. Petersburg 194021, Russia
(Received 4 December 1997)

The energetics of multisheet arrays of two-dimensional islands is studied where the structure of the surface sheet is determined by thermodynamic equilibrium under the constraint of a fixed structure of sheets of buried islands. For the arrangement of islands in a single surface sheet, both a one-dimensional structure of stripes and a two-dimensional structure of square-shaped islands are examined. The buried islands are considered as planar elastic defects characterized by a uniaxially anisotropic double force density, and the surface islands are considered as two-dimensional islands characterized by an isotropic intrinsic surface stress tensor. It is shown that, in cubic crystals with a negative parameter of elastic anisotropy, $\xi=(c_{11}-c_{12}-2c_{44})/c_{44}<0$, the elastic interaction between successive sheets of islands parallel to the (001) crystallographic plane exhibits an oscillatory decay with the separation between sheets. This oscillatory decay is related to generalized Rayleigh waves in elastically anisotropic crystals. By varying the distance between successive sheets of islands, a transition occurs from vertical correlations between islands where islands of the upper sheet are formed above the buried islands of the lower sheet to *anticorrelations* between islands where islands of the upper sheet are formed above the spacings in the lower sheet. The separation between successive sheets of islands corresponding to this transition depends drastically on the anisotropy of the double force density of buried islands. Thus an explanation for the recently observed anticorrelations in multisheet arrays of CdSe islands in the ZnSe matrix is obtained. [S0163-1829(98)04619-0]

I. INTRODUCTION

Recent breakthroughs in quantum wire and quantum dot fabrication relies considerably on effects of spontaneous formation of ordered nanostructures.[1–8] The latter include (i) single-sheet ordered arrays of two-dimensional (2D) islands formed, e.g., in heteroepitaxial systems upon submonolayer deposition;[9–11] (ii) single-sheet ordered arrays of three-dimensional (3D) coherently strained islands formed in highly lattice-mismatched heteroepitaxial systems;[12–22] (iii) multisheet arrays of 3D coherently strained islands ordered both in the lateral plane and in the vertical direction;[12,23–31] (iv) composition-modulated structures in semiconductor alloy films revealing lateral superlattices,[32] vertical superlattices,[33–35] arrays of quantum wires, or quantum dots.[36,37] Recently, multisheet arrays of 2D islands have been fabricated.[38]

In the field of spontaneous formation of ordered semiconductor nanostructures, two possibilities are traditionally distinguished. First, *equilibrium domain structures* can be formed in *closed systems*. Such formation is realized by long-time growth interruption or by post-growth annealing. Thermodynamics can be applied to describe the equilibrium structures that meet the conditions of the Helmholtz free energy minimum. Second, *nonequilibrium structures* can be formed in *open systems*. Such structures are formed in the growth process and observed *in situ* or *ex situ* in *as-grown samples*. The structures are additionally governed by growth kinetics.

Multisheet arrays of islands are distinct from other types of nanostructures for the two following reasons.

First, formation of multisheet arrays of 2D or 3D islands is a process that is dominated by both equilibrium ordering and kinetic-controlled ordering. If the deposition of the first sheet of islands of material 2 on a material 1 is followed by a growth interruption, or just the growth rate is sufficiently low, islands of the equilibrium structure are formed. If then islands are regrown by material 1, and the second cycle of the deposition of material 2 is introduced, a new growth mode occurs. For typical growth temperatures and growth rates, the structure of the buried islands of the first sheet does not change during the deposition of the second sheet. The second sheet of islands grows *in the strain field created by the buried islands of the first sheet*. And the structure of the second sheet of islands reaches the equilibrium *under the constraint of the fixed structure of buried islands of the first sheet*.

Second, a variation of the separation between successive sheets gives an additional possibility (as compared to single-sheet arrays) to tune geometrical and electronic characteristics of nanostructures.

A remarkable feature of multisheet arrays of 3D islands is that the buried islands in successive sheets are spatially correlated. At the surface, new islands were observed to be formed directly above buried islands. The existing theory explaining well the correlation is based on accounting the strain created by buried islands. In Refs. 25 and 26, the strain-induced migration of adatoms of the growing layer was shown to drive adatoms to positions above buried islands. In Ref. 28, energetically preferred sites for nucleation of islands of the second sheet were shown to occur above buried islands. In above papers, buried islands were approxi-

mated as elastic point defects, and the crystal was treated as an elastically isotropic medium.

In seeming contradiction to the above experimental and theoretical results, very recent experiments on multisheet arrays of 2D islands of CdSe in the ZnSe matrix[39] unambiguously and surprisingly revealed vertical *anticorrelation* between islands in successive sheets. Surface islands are formed above the spacings in the sheet of buried islands.

Motivated by these observations, we examine here in detail the energetics of multisheet arrays of 2D islands and seek the equilibrium configuration of the array of surface islands, under the constraint of a fixed array of buried islands. The two key experimental and theoretical inputs of our treatment that make it different from both those of Xie *et al.*[25,26] and that of Tersoff *et al.*[28] are as follows.

First, we consider 2D islands of 1–2 monolayers (ML) height,[39] where the separation between successive sheets is comparable to or even less than the lateral size of the islands in the (xy) plane. We take into account their exact shape.

Second, elastic anisotropy of cubic crystals is known to favor the ordering of nanostructures in elastically soft directions,[1,4,5,18] and one can expect a significant effect of elastic anisotropy on vertical correlations between islands.

Since a single-sheet array of 2D islands can exist in two qualitatively different forms, namely as a one-dimensional array of stripes or as a two-dimensional array of disks,[40,41] both possibilities are addressed in the paper.

II. BASIC EQUATIONS

The key mechanism responsible for the relative arrangement of islands in successive sheets is the formation of an equilibrium array of surface islands in the strain field of buried islands. To extract the essential physics governing the anticorrelation, it suffices to examine a double-sheet array that is comprised of one sheet of buried islands and one sheet of surface islands. The further extension to an arbitrary number of sheets is then very straightforward.

Let material 2 be deposited on the (001) surface of the cubic substrate 1. Upon submonolayer deposition, a periodic array of monolayer-height islands is formed.[2,3,40,41] Let the structure then be regrown by the substrate material 1, and introduce the second cycle of deposition of material 2. The total energy of the surface array of islands in the strain field of the buried islands is

$$E_{\text{total}} = E_{\text{surf}} + E_{\text{boundaries}} + \Delta E^{(SS)}_{\text{elastic}} + E^{(SB)}_{\text{elastic}}. \qquad (2.1)$$

Here, E_{surf} is the sum of the surface energy of surface islands and of the surface energy of uncovered parts of material 1, $E_{\text{boundaries}}$ is the energy of island boundaries, $\Delta E^{(SS)}_{\text{elastic}}$ is the elastic relaxation energy of surface (S) islands due to the discontinuity of the intrinsic surface stress tensor on island boundaries,[2,3] $E^{(SB)}_{\text{elastic}}$ is the elastic energy of the interaction of surface islands (S) and of buried islands (B). Since we address effects of the finite lateral size of islands and of elastic anisotropy and avoid other complications, we focus on the typical experimental situation of *an equal amount of the deposited material in each deposition cycle*. Then each sheet of islands alone tends to form the *same periodic structure*, which corresponds to the minimum of the sum of the first three terms on the right-hand side of Eq. (2.1). If the interaction between the surface islands and the buried islands is neglected, the surface array of islands *as a whole* can be subject to an arbitrary shift in the xy plane. The strain field created by buried islands has the same periodicity as the array of surface islands alone. Therefore, the fourth term in Eq. (2.1) does not change the periodicity of the surface structure, and just defines its *relative position with respect to the array of buried islands* (Fig. 1). Since the interaction energy $E^{(SB)}_{\text{elastic}}$ is the only term in Eq. (2.1) that depends on the shift of the array of surface islands as a whole with respect to the buried islands, we will focus on this energy term only. Below, we will derive the dependence of $E^{(SB)}_{\text{elastic}}$ on the shift X_0 for a 1D array of stripes [Fig. 1(a)] and on the shifts X_0 and Y_0 for a 2D array of compact islands. For simplicity, we will consider the extreme case of compact islands distinct from

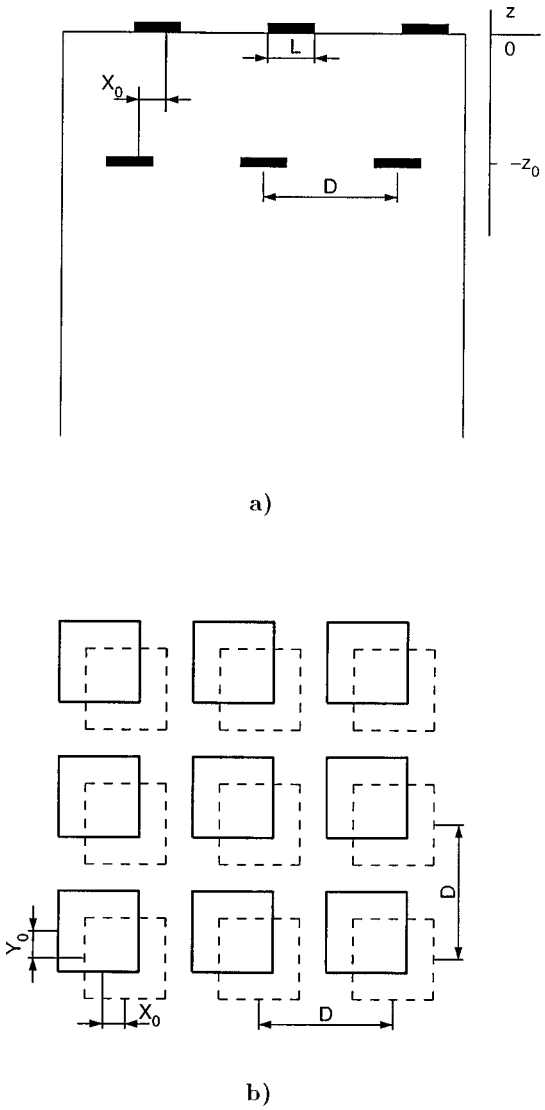

FIG. 1. Geometry of double-sheet arrays of two-dimensional islands. The array of surface islands has the same structure as the array of buried islands but is shifted as a whole. (a) Each sheet of islands forms a one-dimensional array of stripes. The cross section of the double-sheet structure is shown. (b) Each sheet of islands forms a two-dimensional array of square-shaped islands. The plan view of the double-sheet structure is plotted. Buried islands are depicted by dashed lines, and solid lines are used for surface islands.

infinitely elongated stripes, namely, square-shaped islands [Fig. 1(b)].

A. Elastic interaction in a system of macroscopic coherent inclusions

If all three dimensions of the islands are large compared to the lattice parameter a, the islands can be treated as macroscopic coherent inclusions in a matrix. For planar islands this condition reads

$$a \ll h \ll L, \tag{2.2}$$

where L is the lateral dimension of the islands and h is their height. Macroscopic coherent inclusions in a matrix are characterized by the stress-free strain $\varepsilon_{ij}^{(0)}$, which refers to the difference between the unit cell of the inclusion material and the unit cell of the matrix material. For a cubic inclusion in a cubic matrix, $\varepsilon_{ij}^{(0)}=(\Delta a/a)\delta_{ij}$, where $(\Delta a/a)$ is the relative lattice mismatch, $\delta_{ij}=1$ if $i=j$, and $\delta_{ij}=0$ otherwise. The spatial distribution of inclusions can be described by the shape function of the inclusions $\vartheta(\mathbf{r})$ defined by

$$\vartheta(\mathbf{r})=\begin{cases}1 & \text{if } \mathbf{r} \text{ is inside the inclusion}\\ 0 & \text{otherwise.}\end{cases} \tag{2.3}$$

To provide coherent conjugation between inclusions and the matrix, additional strain appears in the heterophase system, and the elastic stress $\sigma_{ij}(\mathbf{r})$ is proportional to the deviation of the strain from stress-free strain,[1]

$$\sigma_{ij}(\mathbf{r})=\lambda_{ijlm}[\varepsilon_{lm}(\mathbf{r})-\varepsilon_{lm}^{(0)}\vartheta(\mathbf{r})]. \tag{2.4}$$

We assume, for simplicity, that the elastic modulus tensors λ_{ijlm} of the matrix and of the inclusions are equal. Then the elastic displacement field $u_i(\mathbf{r})$ obeys the following equilibrium equation of the elasticity theory:[1]

$$\lambda_{ijlm}\nabla_j\nabla_l u_m(\mathbf{r})=\nabla_j[\sigma_{ij}^{(0)}\vartheta(\mathbf{r})], \tag{2.5}$$

where the tensor $\sigma_{ij}^{(0)}$ is connected with the stress-free strain $\varepsilon_{ij}^{(0)}$ as follows:

$$\sigma_{ij}^{(0)}=\lambda_{ijlm}\varepsilon_{lm}^{(0)}. \tag{2.6}$$

The physical meaning of the tensor $\sigma_{ij}^{(0)}$ can be elucidated if one substitutes $\vartheta(\mathbf{r})=\int d^3\mathbf{r}\ \delta(\mathbf{r}-\tilde{\mathbf{r}})\vartheta(\tilde{\mathbf{r}})$ into Eq. (2.5). Then Eq. (2.5) takes the following form:

$$\lambda_{ijlm}\nabla_j\nabla_l u_m(\mathbf{r})=\int d^3\tilde{\mathbf{r}}\ \nabla_j[\sigma_{ij}^{(0)}\delta(\mathbf{r}-\tilde{\mathbf{r}})]\vartheta(\tilde{\mathbf{r}}). \tag{2.7}$$

The integrand on the right-hand side of Eq. (2.7) does not vanish inside inclusions, and the quantity

$$f_i(\mathbf{r})=\sigma_{ij}^{(0)}\nabla_j\delta(\mathbf{r}-\tilde{\mathbf{r}}) \tag{2.8}$$

may be regarded as the *body force density* existing at each point inside the inclusions. The particular form of the body force density (2.8) corresponds to a *superposition of three mutually perpendicular double forces without moment centered at the point* $\tilde{\mathbf{r}}$.[42,43] In this sense, the tensor $\sigma_{ij}^{(0)}$ has the meaning of the *double force density* characterizing the given inclusion. To avoid confusion it is worth noting that the ''body force density'' is the vector $\nabla_j[\sigma_{ij}^{(0)}\vartheta(\mathbf{r})]$ while the ''double force density'' is the second-rank tensor $\sigma_{ij}^{(0)}\vartheta(\mathbf{r})$.

For more than one type of inclusion, the tensor $\sigma_{ij}^{(0)}$ and $\varepsilon_{ij}^{(0)}$ depend on the type of inclusions p. The elastic energy of interacting inclusions may be written in the form where shape functions of the inclusions enter explicitly,[1]

$$\begin{aligned}E_{\text{elastic}}&=\sum_p\ \frac{1}{2}\int d^3\mathbf{r}\ \sigma_{ij}^{(0)p}\vartheta_p(\mathbf{r})[\varepsilon_{ij}^{(0)p}-\varepsilon_{ij}(\mathbf{r})]\\ &=\sum_p\ \frac{1}{2}\int d^3\mathbf{r}\ \sigma_{ij}^{(0)p}\varepsilon_{ij}^{(0)p}\vartheta_p(\mathbf{r})\\ &\quad-\sum_{p,q}\ \frac{1}{2}\int d^3\mathbf{r}\int d^3\mathbf{r}'\,\sigma_{ij}^{(0)p}\vartheta_p(\mathbf{r})\nabla_j\\ &\quad\times G_{il}(\mathbf{r},\mathbf{r}')\nabla'_m\sigma_{lm}^{(0)q}\vartheta_q(\mathbf{r}').\end{aligned} \tag{2.9}$$

Here, $G_{il}(\mathbf{r},\mathbf{r}')$ is the static Green's tensor of the elasticity theory defined for a given crystal and obeying stress-free boundary conditions on the surfaces.[44]

Since we focus on planar islands that obey the inequality (2.2) the height of the islands is the smallest dimension in the system. Then, the equation for the elastic energy (2.9) can be simplified. First, we integrate over $\mathbf{r}'$ by parts and use for the shape function of the islands the following equations:

$$\vartheta^B(\mathbf{r})=h^B\Theta^B(\mathbf{r}_\parallel)\delta(z+z_0), \tag{2.10a}$$

$$\vartheta^S(\mathbf{r})=h^S\Theta^S(\mathbf{r}_\parallel)\delta(z). \tag{2.10b}$$

Here superscripts B and S refer to buried and surface islands, respectively, $\mathbf{r}_\parallel=(x,y)$ is the 2D position vector. $\Theta^B(\mathbf{r}_\parallel)$ and $\Theta^S(\mathbf{r}_\parallel)$ are 2D shape functions. For planar islands obeying the inequality (2.2), one may approximate that the stress-free boundary conditions on the surface are imposed on the $z=0$ plane. Then, for the Green's tensor $G_{il}(\mathbf{r},\mathbf{r}')$ one may use the Green's tensor for a semi-infinite crystal bounded by a stress-free planar surface $z=0$, $G_{il}(\mathbf{r}_\parallel-\mathbf{r}'_\parallel;z,z')$. By substituting Eqs. (2.10a) and (2.10b) into Eq. (2.9), and extracting only the energy of interaction of the surface islands and of the buried islands, one obtains the interaction energy per unit surface area as follows:

$$E^{(SB)}_{\text{elastic}}=\frac{h^S h^B}{A}\int d^2\mathbf{r}_\parallel \int d^2\mathbf{r}'_\parallel \Theta^S(\mathbf{r}_\parallel)\sigma^{(0)S}_{ij}[\nabla_j\nabla'_m G_{il}(\mathbf{r}_\parallel - \mathbf{r}'_\parallel ;z,z')]\Big|_{\substack{z=0\\ z'=-z_0}} \sigma^{(0)B}_{lm}\Theta^B(\mathbf{r}'_\parallel), \tag{2.11}$$

where A is the total surface area.

Since the islands in the two sheets form identical periodic structures shifted by $\mathbf{R}_0=(X_0,Y_0)$, it is convenient to use the Fourier series expansion for the shape functions,

$$\Theta^B(\mathbf{r})=\sum_{\mathbf{k}_\parallel}\widetilde{\Theta}(\mathbf{k}_\parallel)\exp(i\mathbf{k}_\parallel\cdot\mathbf{r}_\parallel), \tag{2.12a}$$

$$\Theta^S(\mathbf{r})=\sum_{\mathbf{k}_\parallel}\widetilde{\Theta}(\mathbf{k}_\parallel)\exp(-i\mathbf{k}_\parallel\cdot\mathbf{R}_0)\exp(i\mathbf{k}_\parallel\cdot\mathbf{r}_\parallel), \tag{2.12b}$$

where the summation is carried out over the reciprocal-lattice corresponding to a periodic structure of the single sheet of islands. By substituting Eqs. (2.12a) and (2.12b) into Eq. (2.11), one obtains the interaction energy in the form of the sum over the reciprocal-lattice vectors,

$$E^{SB}_{\text{elastic}}=h^B h^S\sum_{\mathbf{k}_\parallel}|\widetilde{\Theta}(\mathbf{k}_\parallel)|^2\exp(i\mathbf{k}_\parallel\cdot\mathbf{R}_0)\sigma^{(0)S}_{ij}[\nabla_j\nabla'_m\widetilde{G}_{il}(\mathbf{k}_\parallel;z,z')]\Big|_{\substack{z=0\\ z'=-z_0}}\sigma^{(0)B}_{lm}, \tag{2.13}$$

where $\nabla_x\equiv ik_x$, $\nabla'_x\equiv -ik_x$, $\nabla_y\equiv ik_y$, and $\nabla'_y\equiv -ik_y$. Since we intend to apply our approach mainly to III-V and II-VI semiconductors having the zinc-blende structure, we consider the crystal as elastically anisotropic cubic medium and use the Fourier transform of the static Green's tensor $\widetilde{G}_{il}(\mathbf{k}_\parallel;z,z')$ obtained by Portz and Maradudin.[44] For the double force density $\sigma^{(0)}_{ij}$ we take the tensor with the uniaxial symmetry,

$$\sigma^{(0)S,B}_{ij}=\begin{pmatrix}\sigma^{(0)S,B}_\parallel & 0 & 0\\ 0 & \sigma^{(0)S,B}_\parallel & 0\\ 0 & 0 & \sigma^{(0)S,B}_\perp\end{pmatrix}=\sigma^{(0)S,B}_\parallel\begin{pmatrix}1&0&0\\0&1&0\\0&0&P^{S,B}\end{pmatrix}, \tag{2.14}$$

where P is the anisotropy parameter of the double force density. The substitution of Eqs. (2.14) and of the explicit form of the Green's tensor from Ref. 44 into Eq. (2.13) yields the interaction energy

$$E^{SB}_{\text{elastic}}=h^S h^B\sigma^{(0)S}_\parallel\sigma^{(0)B}_\parallel\sum_{\mathbf{k}_\parallel}|\widetilde{\Theta}(\mathbf{k}_\parallel)|^2\exp(i\mathbf{k}_\parallel\cdot\mathbf{R}_0)k_\parallel \times\sum_{s=1}^{3}Q^{\text{uniaxial}}_s(P^S,P^B;\varphi)\exp(-\alpha_s(\varphi)k_\parallel z_0). \tag{2.15}$$

Here $s=1,2,3$ labels static analogs of Rayleigh waves contributing to the Green's tensor $\widetilde{G}_{il}(\mathbf{k}_\parallel;z,z')$, $\alpha_s(\varphi)$ are dimensionless attenuation coefficients of these waves, and φ is the angle between the $\mathbf{k}_\parallel$ vector and [100] crystallographic direction. Coefficients Q_s for cubic inclusions ($P^S=P^B=1$) were obtained elsewhere.[45,46] Explicit definition of Q_s for arbitrary P^B and P^S is given in Appendix A.

B. Interactions between monolayer-height islands

The above equations are derived for macroscopic coherent inclusions in the matrix, where all dimensions of inclusions are large compared to the lattice parameter. To extend our approach to monolayer-thick inclusions, we refer to the macroscopic description of the strain field created by point defects.[42] A point defect located at $\tilde{\mathbf{r}}$ is represented by the superposition of three mutually perpendicular double forces, and the effective body force density is

$$f_i(\mathbf{r})=a_{ij}\nabla_j\delta(\mathbf{r}-\tilde{\mathbf{r}}). \tag{2.16}$$

A monolayer-thick inclusion with macroscopic dimensions is a two-dimensional array of point defects occupying each atomic site within a certain area. The latter can be described by a two-dimensional shape function $\Theta^B(\mathbf{r}_\parallel)$. The body force density associated with the given inclusion can be obtained by adding contributions of single point defects from Eq. (2.16). In the macroscopic approach, this summation can be replaced by integration, i.e.,

$$f_i(\mathbf{r})=\frac{1}{A_0}\int d^2\tilde{\mathbf{r}}_\parallel a_{ij}\nabla_j[\delta(\mathbf{r}_\parallel-\tilde{\mathbf{r}}_\parallel)\delta(z-\tilde{z})]\Theta^B(\tilde{\mathbf{r}}_\parallel), \tag{2.17}$$

where A_0 is unit cell area in the xy plane. Two expressions for the double force density, a macroscopic one from Eq. (2.8) and a microscopic one from Eq. (2.17), coincide if one sets $\sigma^{(0)}_{ij}=a_{ij}/v$, where v is the unit cell volume.

Equation (2.17) is derived under the assumption of no mutual influence between the point defects comprising the inclusion. Generally speaking, the tensor a_{ij} characterizing the double force density is different for a single point defect and for a monolayer-thick inclusion. A substitutional impurity atom in a zinc-blende crystal of III-V or II-VI semiconductor has T_d site symmetry, and the corresponding double-force tensor a_{ij} has cubic symmetry. On the other hand, if the inclusion of equal substitutional impurity atoms is oriented in the (001) plane of the zinc-blende crystal, has mono-

layer thickness, and infinite lateral dimensions, each atom of the inclusion has D_{2d} symmetry. Therefore, the tensors a_{ij} and $\sigma_{ij}^{(0)}$ characterizing the double force density of a buried island of a monolayer-thickness have *uniaxial symmetry*. With the increase of the thickness of the inclusion, components $\sigma_{\parallel}^{(0)}$ and $\sigma_{\perp}^{(0)}$ depend on the thickness. For an inclusion with three macroscopic dimensions, the tensor $\sigma_{ij}^{(0)}$ becomes related to the stress-free strain $\varepsilon_{ij}^{(0)}$ via Eq. (2.6). For an inclusion of a cubic material in a cubic matrix, the tensor $\sigma_{ij}^{(0)}$ reduces then to an isotropic one, $\sigma_{ij}^{(0)}=(c_{11}+2c_{12})(\Delta a/a)\delta_{ij}$, where c_{11} and c_{12} are elastic moduli in the Voigt notation.

The above discussion shows that the double force density $\sigma_{ij}^{(0)}$ has clear physical meaning even for inclusions of 1 ML thickness, whereas the stress-free strain $\varepsilon_{ij}^{(0)}$ is defined only for macroscopic inclusions. This is why we are using $\sigma_{ij}^{(0)}$ as the main characteristic of inclusions in the present paper.

The energy of the surface island in the strain field can be described in terms of the *intrinsic surface stress tensor*.[47] The crystal surface partially covered by monolayer-height islands can be regarded as a system of two distinct phases 1 and 2, where the phase 1 is the bare surface of material 1 and the phase 2 is the complex surface of a monolayer-height island of material 2 on the substrate of material 1. These two phases are characterized by different intrinsic surface stress tensors, $\tau_{\alpha\beta}^{(1)}$ and $\tau_{\alpha\beta}^{(2)}$, $\{\alpha,\beta\}=\{x,y\}$. Then the strain-dependent contribution to the surface energy equals

$$\Delta E_{\text{surface}}=\int d^3\mathbf{r}_{\parallel}\Theta^S(\mathbf{r}_{\parallel})\tau_{\alpha\beta}^{(2)}\varepsilon_{\alpha\beta}(\mathbf{r}_{\parallel},z)\big|_{z=0}+\int d^2\mathbf{r}_{\parallel}[1-\Theta^S(\mathbf{r}_{\parallel})]\tau_{\alpha\beta}^{(1)}\varepsilon_{\alpha\beta}(\mathbf{r}_{\parallel},z)\big|_{z=0}. \tag{2.18}$$

To reveal the energy of the interaction of surface islands and of buried islands, one should keep in Eq. (2.18) only terms containing the shape function $\Theta^S(\mathbf{r}_{\parallel})$ and to retain in the strain $\varepsilon_{\alpha\beta}(\mathbf{r}_{\parallel},\ z=0)$ only its part due to buried islands, $\varepsilon_{\alpha\beta}^{B}(\mathbf{r}_{\parallel},\ z=0)$. This yields

$$E_{\text{elastic}}^{SB}=\int d^2\mathbf{r}_{\parallel}\Theta^S(\mathbf{r}_{\parallel})(\Delta\tau_{\alpha\beta})\varepsilon_{\alpha\beta}^{B}(\mathbf{r}_{\parallel},z)\big|_{z=0}, \tag{2.19}$$

where $(\Delta\tau_{\alpha\beta})=\tau_{\alpha\beta}^{(2)}-\tau_{\alpha\beta}^{(1)}$.

To establish the connection between the energy of elastic interaction of two arrays of islands written in terms of the double force density $\sigma_{ij}^{(0)}$ (2.9), and the energy written in terms of the intrinsic surface stress (2.19), it is necessary to reduce the energy of Eq. (2.9) to a form where only in-plane components $\varepsilon_{\alpha\beta}^{B}(\mathbf{r}_{\parallel},z)$ enter. Since the surface $z=0$ is a stress-free one, the corresponding boundary conditions allow us to express all components of the strain tensor in terms of $\varepsilon_{\alpha\beta}^{B}(\mathbf{r}_{\parallel},z)$ only. This procedure carried out in Appendix B yields the energy E_{elastic}^{SB} as follows:

$$E_{\text{elastic}}^{SB}=h^S\int d^2\mathbf{r}_{\parallel}\Theta^S(\mathbf{r}_{\parallel})\widetilde{\sigma_{\alpha\beta}}\varepsilon_{\alpha\beta}^{B}(\mathbf{r}_{\parallel},z)\big|_{z=0}, \tag{2.20}$$

where $\widetilde{\sigma_{\alpha\beta}}$ are in-plane components of the stress tensor in the uniform flat film of material 2 coherently conjugated to the substrate of material 1. Equation (2.19) formally coincides with Eq. (2.20) if one sets

$$\Delta\tau_{\alpha\beta}=\widetilde{\sigma_{\alpha\beta}}h^S. \tag{2.21}$$

However, although the intrinsic surface stress $\tau_{\alpha\beta}$ can be qualitatively modeled as bulk stress in the epitaxial layer, Eq. (2.21) does not hold quantitatively. The substrate surface covered with a monolayer-thick epitaxial layer is, strictly speaking, a completely new surface distinct from both the substrate surface and the surface of the deposited material. This complex surface has its own surface energy and its own intrinsic surface stress tensor.

Nevertheless, apart from special cases where the discontinuity of the intrinsic surface stress tensor $\Delta\tau_{\alpha\beta}$ differs significantly from Eq. (2.21) (see, e.g., Ref. 50), in many lattice-mismatched heteroepitaxial systems Eq. (2.21) yields the correct sign and the correct order of magnitude of $\Delta\tau_{\alpha\beta}$. To clarify the physical reason for it, we make a rough estimate of the right-hand side of Eq. (2.21), by setting $\widetilde{\sigma_{\alpha\beta}}h\approx Y\varepsilon_0 h$, where Y is Young's modulus, ε_0 is the lattice mismatch, and a is the lattice parameter. The substitution of $Y\approx 500$ meV Å^{-3}, $\varepsilon_0\approx 0.07$, and $a=3$ Å yields ≈ 100 meV Å^{-2}, which is of the order of the characteristic value of τ for surfaces of pure crystals, where $\tau\sim 100$ meV Å^{-2}.[48,49]

Below we assume that Eq. (2.21) holds for the system in question. The above arguments show that this assumption gives in most cases the correct sign and the order of magnitude of the interaction energy. The former will enable us to obtain the correct relative arrangement of the two sheets of islands, whereas the latter will allow us to compare the characteristic energy with other typical energies involved in the spontaneous formation of surface domain structures.

Besides that, it follows from Eq. (2.20) that $\widetilde{\sigma_{\alpha\beta}}$ is the only quantity that depends on the characteristics of the surface island, particularly, on the parameter P^S referring to the anisotropy of the double force density associated with this island. Therefore, the variation of P^S would result only in the variation of the common factor in the energy (2.20) independent of the separation z_0 between layers, and of the relative shift (X_0,Y_0) of the two arrays. Moreover, for monolayer-thick surface islands, the quantity P^S is irrelevant since the surface islands are characterized by the *planar tensor* $\Delta\tau_{\alpha\beta}$.

It follows from the above discussion that it is possible to describe the interaction between the two sheets of islands by Eq. (2.15) and to set $P^S=1$. Then the anisotropy of the double force density of *buried islands* P^B is the only key parameter that governs the elastic interaction between the two sheets of islands.

III. ONE-DIMENSIONAL ARRAYS OF STRIPES

Since most of the essential physics can be understood in the example of a one-dimensional array of stripes, we present first the detailed analysis of the 1D case. The orientation of stripes is governed by the anisotropy of the intrinsic surface stress tensor $\tau_{\alpha\beta}$, on the one hand, and by the anisotropy of the bulk elastic modulus tensor λ_{ijlm}, on the other hand. The principal axes of the tensor $\tau_{\alpha\beta}$ are [110] and [1$\bar{1}$0] directions and this anisotropy promotes the orientation of stripes in one of these directions, whereas the anisotropy of the bulk

elastic modulus tensor favors the orientation of spontaneously ordered structures in the elastically soft directions [100] and [010]. Both orientations are observed in experiment. InAs striped islands on GaAs(001) under submonolayer coverage are oriented in the [110] direction,[9,10] whereas a larger than 1-ML coverage in the same system reveals nonplanar morphology with islands elongated in the [100] direction.[11] In the present study of stripe-shaped islands, we will consider both of these symmetries. For both cases, stripes are oriented perpendicular to a mirror plane, and the elastic displacement field created by islands contains only sagital displacements in the mirror plane, whereas transverse displacements vanish.

Since we intend to apply our consideration mainly to III-V and II-VI semiconductors with zinc-blende structure, we consider the crystal as elastically anisotropic cubic medium with a negative parameter of elastic anisotropy,

$$\xi=\frac{c_{11}-c_{12}-2c_{44}}{c_{44}}<0. \tag{3.1}$$

The crucial consequence of the negative ξ is that the dimensionless coefficients of static analogs of Rayleigh waves $\alpha_s(\varphi)$, which govern the dependence of the interaction energy (2.15) on the separation between the two layers, are complex. Particularly, evaluation of α_s for each direction of the wave vector $\mathbf{k}_\parallel$ by means of Eq. (2.16) of Ref. 44 yields that two coefficients are complex conjugate,

$$\alpha_{1,2}=\alpha'\pm i\alpha'', \tag{3.2}$$

where the sign + or − stands for α_1 or α_2, respectively, and the third coefficient is real, $\alpha_3^*(\varphi)=\alpha_3(\varphi)$. Complex attenuation coefficients α imply that *the static analogs of Rayleigh waves exhibit not purely an exponential decay, but an oscillatory one*. This phenomenon is known for surface acoustic waves which are *generalized Rayleigh waves* in elastically anisotropic crystal.[51,52] The complex attenuation coefficients lead to the conclusion that the elastic interaction between successive sheets of islands exhibits an oscillatory decay with the separation between sheets.

To discuss the impact of this oscillatory decay on the mutual arrangement of two successive sheets of islands, it is worthwhile to consider the simplest model where the Fourier expansion of the shape function of the islands (2.12a) contains a single Fourier harmonics,

$$\Theta(\mathbf{r}_\parallel)=\Theta_1\cos\left(\frac{2\pi x}{D}\right), \tag{3.3}$$

and stripe-shaped islands are oriented perpendicular to the (010) mirror plane of the crystal. Then, by evaluating Q_s^{uniaxial} for this orientation, and by substituting it into Eq. (2.15), one obtains the interaction energy as a function of the shift X_0 and of the depth of the layer of buried islands, z_0,

$$E_{\text{elastic}}^{SB}=-h^2(\Theta_1)^2\,\frac{\pi}{D}\,\frac{(\sigma_\parallel^{(0)})^2}{c_{44}\alpha''}\,R\,\cos\left[\frac{2\pi X_0}{D}\right]\times\sin\left[\Phi_0-\alpha''\,\frac{2\pi z_0}{D}\right]\exp\left[-\alpha'\,\frac{2\pi z_0}{D}\right]. \tag{3.4}$$

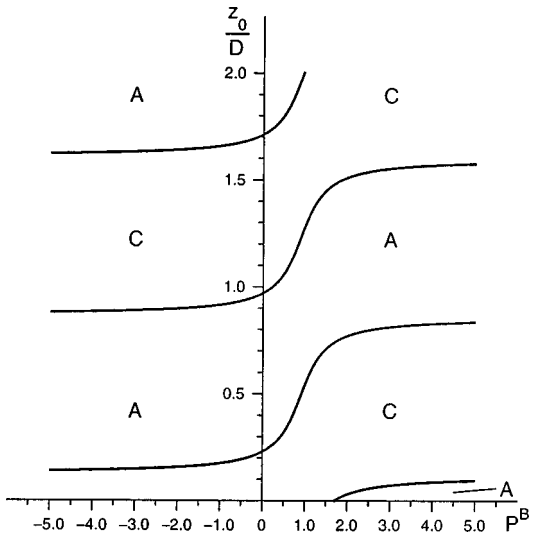

FIG. 2. The model phase diagram of the elastic interaction between the array of surface stripe-shaped islands and the array of buried stripe-shaped islands. The phase diagram is constructed for the model one-dimensional sinusoidal shape function of the islands, $\Theta(\mathbf{r}_\parallel)\sim\cos(\mathbf{k}_\parallel\cdot\mathbf{r}_\parallel)$. P^B is the anisotropy of the double force density of buried islands. z_0 is the separation between the surface and the sheet of buried islands, and D is the period. C denotes vertical correlation, and A denotes vertical anticorrelation. The modulation of the density occurs in the [100] direction, $\mathbf{k}_\parallel\|[100]$.

Here R and Φ_0 are the absolute value and the phase of the quantity,

$$1-\frac{(c_{12}+c_{44})(1+P^B\alpha_{1,2}^2)}{c_{11}\alpha_{1,2}^2+c_{12}}=R\,\exp(\pm i\Phi_0). \tag{3.5}$$

The dependence of the energy from Eq. (3.4) on the relative shift of two arrays of islands is governed by a single factor $\cos[2\pi X_0/D]$. Therefore, the energy reaches its minimum at $X_0=0$ (correlation), or at $X_0=\pm D/2$ (anticorrelation). The transition from correlation to anticorrelation occurs if the sine in Eq. (3.4) changes its sign. The latter occurs if the thickness of the separation layer z_0 obeys the equation

$$\Phi_0-\alpha''|k_x|z_0=n\pi, \tag{3.6}$$

where n is an arbitrary integer number. These values of z_0 correspond to the transition between correlation and anticorrelation for a model structure where the shape function of the islands contains one Fourier harmonic only. Figure 2 depicts the phase diagram of correlation and anticorrelation, which depends on the anisotropy of the double force density of buried islands, $P^B=\sigma_\perp^{(0)}/\sigma_\parallel^{(0)}$, and on the separation between islands. An important issue of the phase diagram is the very steep slope close to $P^B=1$. It implies that even small deviations from isotropic double force density, i.e., from $P^B=1$, may lead to dramatic changes of the arrangement of

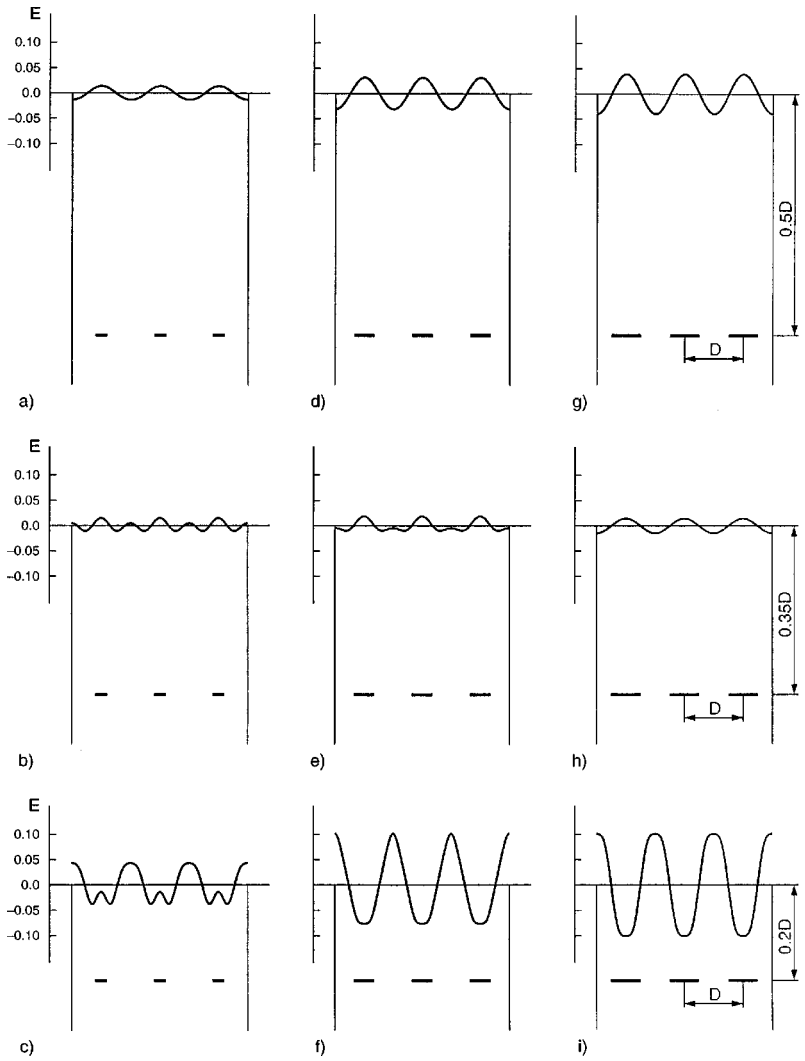

FIG. 3. The interaction energy of a sheet of surface islands and a sheet of buried islands. Both sheets consist of identical one-dimensional arrays of infinitely elongated stripes. The energy is defined per unit surface area and is given in meV Å^{-2}. The width of the islands equals $0.2D$ in (a), (b), and (c); $0.35D$ in (d), (e), and (f); $0.5D$ in (g), (h), and (i).

a multisheet array of islands. The phase diagram for stripes elongated in the [110] direction is very much like the one in Fig. 2.

The shape function of real islands is not a single Fourier harmonic but a rectangular function in real space. For an array of stripes of the width L having the periodicity D, the Fourier transform of the shape function equals

$$\tilde{\Theta}(\mathbf{k}_\parallel)=\frac{2}{D}\frac{\sin(k_x L/2)}{k_x}. \tag{3.7}$$

To perform numerical calculations, we use particular parameters of CdSe:ZnSe islands studied experimentally in Ref. 39. As will be discussed in detail in Sec. V, the islands are $Zn_{1-x}Cd_xSe$ islands having a thickness of 2 ML and the characteristic lateral periodicity of ≈ 100 Å. For the double force density $\sigma_\parallel^{(0)S,B}$ entering Eq. (2.15) we take $\sigma_\parallel^{(0)B}=\sigma_\parallel^{(0)S}=(c_{11}+2c_{12})\varepsilon^{(0)}x$, where $\varepsilon^{(0)}=0.0725$ is the lattice mismatch between bulk CdSe and bulk ZnSe, and $x=0.4$ is the Cd content in the islands. The elastic moduli $c_{11}=0.850\times 10^{12}$ erg cm^{-3}, $c_{12}=0.502\times 10^{12}$ erg cm^{-3}, and $c_{44}=0.407\times 10^{12}$ erg cm^{-3} are taken from Ref. 53. The anisotropy parameter of the double force density P^B is the fitting parameter of the theory. Below we study the dependence of the relative arrangement of the two sheets of islands on the parameter P^B both for 1D arrays of stripes (in this section) and for 2D arrays of square-shaped islands (in Sec. IV). Comparison of our theoretical conclusions with the experimental observations of Ref. 39, which is carried out in Sec. V, gives the interval for the parameter P^B, $P^B \leqslant 0.5$. Here we present a more detailed analysis of the dependence of the relative arrangement of the two sheets of islands on the separation z_0 between the layers and on the coverage $Q=L/D$ by fixing one particular value of $P^B=0.5$.

Figure 3 shows the elastic interaction energy versus the shift X_0 of two successive sheets of islands where results are presented for three different separations z_0 and for three values of the coverage Q. If $z=0.2D$, and the coverage Q equals 0.5 [Fig. 3(i)] or $Q=0.35$ [Fig. 3(f)], vertical correlation occurs. If $Q=0.2$, the plot of the energy versus the shift X_0 has two minima per period. For larger separation between sheets of islands, $z_0=0.35D$, the amplitude of the energy profile decreases, and vertical correlations are replaced by anticorrelation [Fig. 3(h)] or by an intermediate arrangement [Fig. 3(e)]. For a lower coverage $Q=0.2$, an intermediate

arrangement of islands persists [Fig. 3(b)]. For even larger separation, $z_0 = 0.5D$, all three arrays show anticorrelation.

To discuss the numerical values presented in Fig. 3 we compare them with the energy per unit area for a single-sheet structure of islands. By extending the equation derived for elastically isotropic media in Ref. 40, for the (001) surface of the cubic crystal, one obtains the energy per unit area of a single-sheet array of stripes, $E = -\sin(\pi Q)(\Delta\tau)^2 2\alpha' c_{11}(c_{11}^2 - c_{12}^2)^{-1}(\pi D)^{-1}$, where Q is the coverage of the surface. By substituting here $\Delta\tau = (c_{11}+2c_{12})(c_{11}-c_{12})c_{11}^{-1}\varepsilon^{(0)}xh^S$, $Q = 0.5$, and by using the above-mentioned numerical values, one obtains $E = -0.08$ meV Å^{-2}. From this estimate it follows that, if the separation between two sheets z_0 is smaller than $0.5D$, the energy of the interaction between two sheets of islands is of the same order of magnitude as the energy of a single sheet. *This comparison confirms that the elastic interaction between the two sheets of islands can indeed result in vertical correlation or anticorrelation between the two sheets.*

It should be noted that the dependence of E on X_0, which has more than one minimum per period, as in Figs. 3(b), 3(c), and 3(e), may give rise, in principle, to a splitting of surface islands in the external strain field. Numerical tests show, however, that at least at $z_0 \geq 0.2D$, such splitting is not energetically favorable. Below, we do not consider such a possibility.

The onset of the intermediate arrangement of islands in the successive sheets is due to the interplay of different Fourier harmonics of the strain field. Since higher harmonics decrease faster with the separation between the two sheets of islands than the lower ones, higher harmonics are important only in a narrow region of the separation z_0 where the amplitude of the main harmonic vanishes.

Figure 4 demonstrates phase diagrams of a double-sheet array of stripe-shaped islands. Phase diagrams are constructed with respect to variables z_0 and P^B for two different coverages of the surface. Each point on the phase diagram corresponds either to vertical correlation or to vertical anticorrelation, or to an intermediate arrangement. These diagrams also demonstrate that the intermediate arrangement occurs mainly if the separation between sheets is not very large, or just if the system is close to the transition from vertical correlation to vertical anticorrelation.

For the smaller value of the coverage Q [Fig. 4(a)], the amplitude of the first Fourier harmonics decreases, and the role of higher Fourier harmonics increases. Correspondingly, the parameter region on the phase diagram corresponding to an intermediate arrangement is larger for smaller Q.

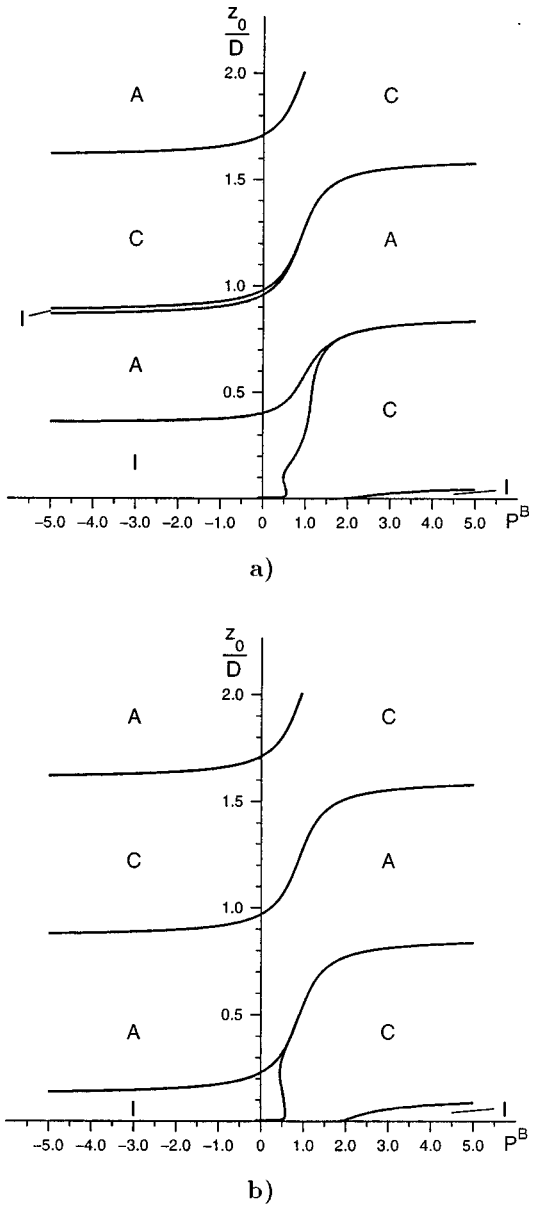

FIG. 4. Phase diagrams of a double-sheet array comprised of an array of surface islands and an array of buried islands. Both arrays are identical one-dimensional arrays of infinitely elongated stripes. Stripes are oriented in the [010] direction. P^B is the anisotropy of the double force density of buried islands, z_0 is the separation between the surface and the sheet of buried islands, and D is the period. C denotes vertical correlation, I denotes an intermediate arrangement and A denotes vertical anticorrelation. (a) The coverage of the surface is 0.2. (b) The coverage of the surface is 0.5.

IV. TWO-DIMENSIONAL ARRAYS OF COMPACT ISLANDS

In this section, we discuss multisheet arrays of 2D islands where each single sheet is a 2D superlattice of compact islands. To reveal the characteristic behavior of such arrays, we focus on such islands that are the most distinct ones from 1D stripes, namely on square-shaped islands. To be specific, we consider square islands oriented in the [100] and [010] directions. For compact islands on the (001) surface of a cubic crystal, the elastic interaction makes a square superlattice the most favorable arrangement.[5] The primitive lattice vectors of the superlattice are oriented in the [100] and [010] directions. Taking into account the anisotropic part of the surface stress tensor could make, under certain circumstances, an asymmetric superlattice more favorable. This complexion is not discussed here.

The symmetry of the system with a square superlattice of buried islands and no surface islands is described by the $P4mm$ layer group. Figure 6(a) depicts seven types of symmetry positions within a unit cell of the superlattice. The

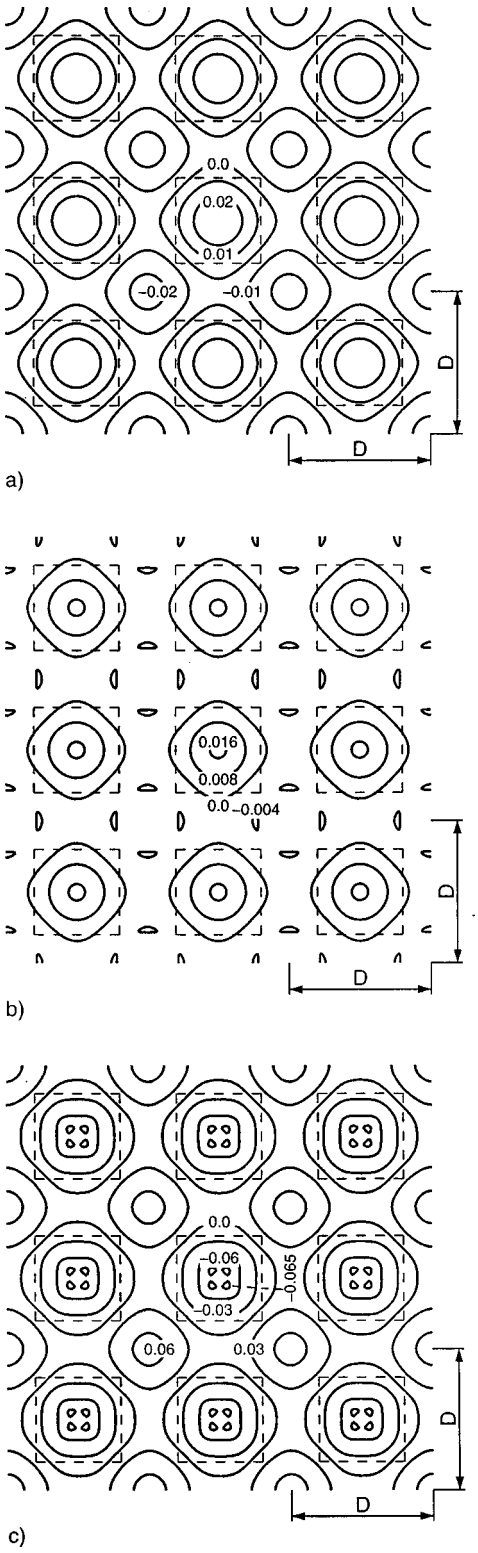

FIG. 5. The interaction energy of an array of surface islands and of an array of buried islands. Both arrays are identical 2D square superlattices of square-shaped islands. The primitive lattice vectors of each superlattice are (1,0,0) and (0,1,0). The energy per unit area is calculated as the function of the relative shift (X_0, Y_0) of two arrays and is given in meV Å^{-2}. The fraction of the surface covered by islands equals 0.35. The separation between sheets of islands equals $0.5D$ for (a), $0.35D$ for (b), and $0.2D$ for (c).

notations of Ref. 54 are used. We will characterize the relative shift of two sheets of islands by the symmetry position of the projection of the center of a surface island onto the superlattice formed by buried islands.

To calculate the energy of interaction between two sheets of islands, we fix the coverage of the surface $Q = L^2/D^2 = 0.35$, and the parameter of the anisotropy of the double force density $P^B = 0.5$. The Fourier transform of the shape function $\Theta(\mathbf{r})$ for square islands equals

$$\tilde{\Theta}(\mathbf{k}_\parallel) = \frac{4}{D^2} \frac{\sin(k_x L/2)}{k_x} \frac{\sin(k_y L/2)}{k_y}. \tag{4.1}$$

We substitute Eq. (4.1) into Eq. (2.13) and calculate the energy as a function of (X_0, Y_0) for several thicknesses of the separation layer z_0. Results are plotted in Fig. 5. For a small thickness of the separation layer, $z_0 = 0.2D$, energy minima correspond to $4d$ symmetry positions close to the $1a$ position [Fig. 5(c)]. Approximately the two sheets of islands exhibit vertical correlation in both [110] and [1$\bar{1}$0] directions. For $z = 0.35$, energy minima correspond to $4f$ positions [Fig. 5(b)], and for $z = 0.5D$ the energy reaches its minimum value at $1b$ positions [Fig. 5(a)], which implies vertical anticorrelation in both [110] and [1$\bar{1}$0] directions.

To give a broader overview of possible relative arrangements of two sheets of islands, we fix the coverage of the surface $Q = 0.35$ and construct the phase diagram in variables $P^B - z_0$. We define the net of parameters P^B and z_0, calculate for each point (P^B, z_0) of the net, the energy versus (X_0, Y_0) and seek the optimum shift (X_0, Y_0) corresponding to the energy minimum. Symmetry of this optimum point is indicated for each region of the phase diagram of Fig. 6(b) according to the definition of Fig. 6(a). For a thin separation layer, $z_0 \leqslant 0.5D$, several types of relative arrangement of two sheets are possible. For thicker separation layer, only main harmonics of the strain field are important. This yields the energy minimum either for vertical correlation (position 1a) or for vertical anti-correlation in both in-plane directions (position 1b).

V. DISCUSSION

The only experimental results on multisheet arrays of 2D islands reported so far are those by Straßburg *et al.*[39] A 20-period vertical superlattice composed of nominally 1.1 monolayer (ML) CdSe insertions separated by 30 Å ZnSe has been grown by molecular beam epitaxy. Structural characterization by cross-section high-resolution transmission electron microscopy (HRTEM) has been performed along the ⟨110⟩ directions. The processing of HRTEM images clearly reveals that the deposited Cd forms a thin layer (1–2 ML) of an alloy $Zn_{1-x}Cd_xSe$ with low Cd content and 2D islands having higher Cd content and lateral dimensions 40–50 Å. The islands in successive sheets exhibit anticorrelation in both (110) and (1$\bar{1}$0) planes.

The results of Ref. 39 show that the islands of each single sheet have a compact shape. The HRTEM reveals contrast modulations of 4 ML height. Here we take into account that the width of contrast modulation can exceed the actual width

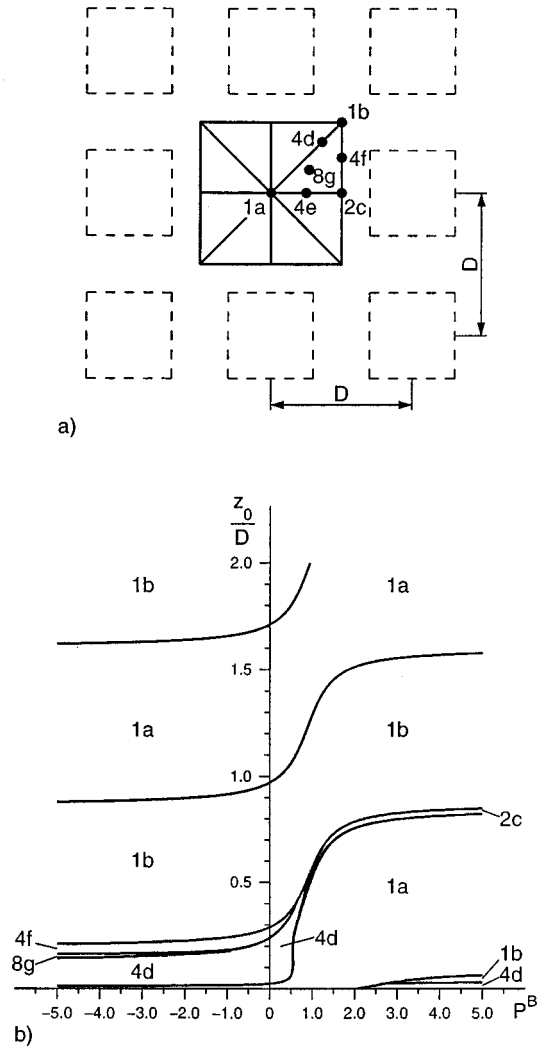

FIG. 6. The phase diagram of a double-sheet array comprised of an array of surface islands and an array of buried islands. Both arrays are identical 2D square superlattices of square-shaped islands. Each square-shaped island is oriented along [100] and [100] directions. The primitive lattice vectors of each superlattice are (1,0,0) and (0,1,0). (a) The relative shift (X_0, Y_0) is defined by the projection of the center of a surface island onto the superlattice formed by the buried islands. This projection is characterized by one of seven types of symmetry depicted in the figure. (b) The phase diagram constructed in variables z_0/D vs P^B. P^B is the anisotropy of the double force density of buried islands, z_0 is the separation between the surface and the sheet of buried islands, and D is the period. Domains of the phase diagram are labeled according to the symmetry of the projection of the center of a surface island onto the superlattice of buried islands, labels being defined in (a).

of islands due to the presence of steps, and we model islands as having 2 ML thickness and a higher Cd content than in the layer between islands. Only the excess content of Cd in islands with respect to the Cd content in the intermediate layer contributes to the inhomogeneous strain field and is responsible for vertical anticorrelation of islands. We take this excess content equal to 40%.

This makes our model of 2D coherent inclusions applicable to the particular experimental situation. Since, on the one hand, the thickness of Cd-rich islands is sufficiently small (2 ML), and, on the other hand, composition of Cd in islands is sufficiently high ($>40\%$), it is reasonable to assume a uniaxially anisotropic double force density associated with the islands. The characteristic periodicity D of Cd-rich islands is about 80–100 Å, leading to a ratio $z_0/Dz_0/D \approx 0.3$–0.4, and the coverage of the surface is in the interval 0.25–0.4. Therefore, the phase diagram of Fig. 6(b) applies to the system in question. The parameter of uniaxial anisotropy $P^B \leqslant 0.5$ matches the experimental results on anticorrelation of islands. Further structural characterization including plan view TEM and cross-section HRTEM for systems with other thickness of separation layer are needed to obtain more information and to extract material parameters of $Zn_{1-x}Cd_xSe$ islands.

VI. SUMMARY

The spontaneous formation of multisheet arrays of two-dimensional inclusions (islands) in a matrix where the structure of each sheet of surface islands is being formed in the strain field of buried islands is studied here. The matrix is described as an elastically anisotropic cubic crystal bounded by a stress-free planar (001) surface, and buried islands are characterized by a uniaxially anisotropic double force density. We have shown that the elastic interaction between a sheet of buried islands and a sheet of surface islands exhibits an oscillatory decay with the thickness of the separation layer, which is related to the existence of generalized Rayleigh waves in elastically anisotropic crystals. By varying the separation between successive sheets of islands, a transition occurs from vertical correlations to vertical anticorrelations in the relative arrangement of islands in successive sheets. The separation corresponding to the transition depends dramatically on the anisotropy parameter of the double force density characterizing buried islands. Phase diagrams are constructed for both 1D arrays of stripes and 2D arrays of compact islands forming each single sheet. The phase diagrams demonstrate a variety of possible arrangements for small separation between successive sheets and reveal a universal behavior for large separation where only vertical correlation or anticorrelation are possible. Our results are in agreement with existing experimental data on anticorrelations in multisheet arrays of 2D islands.

ACKNOWLEDGMENTS

The authors are grateful to Yu. E. Kitaev for drawing their attention to the description of the symmetry of the structure by layer groups and to the usage of correct notations of symmetry positions. The authors thank I. L. Krestnikov for helpful discussions. The work was supported by the Russian Foundation for Basic Research Grant No. 96-02-17943a, by the Joint Grant of the Deutsche Forschungsgemeinschaft (Sfb 296), and of the Russian Foundation for Basic Research (96-02-00168G), and by the Volkswagen Stiftung.

APPENDIX A

The explicit expression for the second derivative of the Green's tensor in Eq. (2.13) is

$$\sigma_{ij}^{(0)S}[\nabla_j\nabla'_m\widetilde{G_{il}}(\mathbf{k}_\parallel;z,z')]\big|_{\substack{z=0\\z'=-z_0}}\sigma_{lm}^{(0)B}=\sigma_{ij}^{(0)S}\sum_{j=1}^{3}\sum_{m=1}^{3}\left[(1-\delta_{j3})ik_j+\delta_{j3}P^S\frac{d}{dz}\right]\times\left[(1-\delta_{m3})(-ik_m)+\delta_{m3}P^B\frac{d}{dz'}\right]\widetilde{G_{il}}(\mathbf{k}_\parallel;z,z')\Big|_{\substack{z=0\\z'=-z_0}}\sigma_{lm}^{(0)B}. \quad \text{(A1)}$$

By substituting the static Green's tensor from Ref. 44 into Eq. (A1), one obtains the equation

$$\sigma_{ij}^{(0)S}[\nabla_j\nabla'_m\widetilde{G_{il}}(\mathbf{k}_\parallel;z,z')]\big|_{\substack{z=0\\z'=-z_0}}\sigma_{lm}^{(0)B}=\sigma_{\parallel}^{(0)S}\sigma_{\parallel}^{(0)B}\Bigg[B_0^{\text{uniaxial}}(P^S,P^B)\,\delta(z-z')+k_\parallel\sum_{s=1}^{3}C_s^{\text{uniaxial}}(P^S,P^B;\varphi)\exp(-\alpha_s k_\parallel|z-z'|)+k_\parallel\sum_{s=1}^{3}\sum_{s'=1}^{3}D_{ss'}^{\text{uniaxial}}(P^S,P^B;\varphi)\exp(-\alpha_s k_\parallel|z|)\exp(-\alpha_{s'}k_\parallel|z'|)\Bigg]\Bigg|_{\substack{z=0\\z'=-z_0}}, \quad \text{(A2)}$$

which extends the corresponding equation for cubic inclusions ($P^S=P^B=1$) obtained in Ref. 4. By substituting $z=0$ and $z'=-z_0$ into the right-hand side of Eq. (A2) and introducing notations

$$Q_s^{\text{uniaxial}}(P^S,P^B;\varphi)=C_s^{\text{uniaxial}}(P^S,P^B;\varphi)+\sum_{s'=1}^{3}D_{s's}^{\text{uniaxial}}(P^S,P^B;\varphi), \quad \text{(A3)}$$

one obtains Eq. (2.15).

APPENDIX B

To establish the connection between two equations for the elastic interaction energy of islands, one for islands of a macroscopic thickness, and another for islands with a monolayer thickness, one should use the boundary conditions on the stress-free surface and express all components of the strain tensor $\varepsilon_{ij}(\mathbf{r}_\parallel,\,z=0)$ in terms of in-plane components $\varepsilon_{\alpha\beta}(\mathbf{r}_\parallel,\,z=0)$ only, where $(\alpha,\beta)=(x,y)$. The procedure is similar to that of Ref. 55 and is carried out as follows.

The interaction energy equals the sum of the energy of surface islands in the strain field of buried islands and of the energy of buried islands in the strain field of surface islands. Due to the reciprocity theorem of elasticity theory, both these energies are equal, and the total interaction energy equals twice the energy of surface islands in the strain field of buried islands. By substituting Eq. (2.10b) into Eq. (2.9), we obtain the interaction energy E_{elastic}^{SB} as follows:

$$E_{\text{elastic}}^{SB}=-h^S\int d^2\mathbf{r}_\parallel\Theta^S(\mathbf{r}_\parallel)\lambda_{ijpq}\varepsilon_{pq}^{(0)}\varepsilon_{ij}^{B}(\mathbf{r}_\parallel,z)\Big|_{z=0}, \quad \text{(B1)}$$

where $\varepsilon_{ij}^{B}(\mathbf{r}_\parallel,z)$ is the contribution to the strain tensor at the surface due to buried islands. This strain obeys the stress-free boundary conditions at the surface, i.e.,

$$\begin{aligned}\sigma_{iz}(\mathbf{r}_\parallel,z)\big|_{z=0}&=\lambda_{izpq}\varepsilon_{pq}(\mathbf{r}_\parallel,z)\big|_{z=0}-\lambda_{izpq}\varepsilon_{pq}^{(0)}\\&=\lambda_{iz\alpha\beta}\varepsilon_{\alpha\beta}^{B}(\mathbf{r}_\parallel,z)\big|_{z=0}+\lambda_{izlz}\varepsilon_{lz}^{B}(\mathbf{r}_\parallel,z)\big|_{z=0}-\lambda_{izpq}\varepsilon_{pq}^{(0)}\\&=0.\end{aligned} \quad \text{(B2)}$$

To find the lz components of the strain tensor $\varepsilon_{ij}(\mathbf{r}_\parallel,z)\big|_{z=0}$ it is convenient to introduce the (3×3) matrix Γ_{il}, which is the inverse matrix to λ_{izlz},

$$\Gamma_{il}\lambda_{lzmz}=\delta_{im}. \quad \text{(B3)}$$

Then the solution of Eq. (B2) yields

$$\varepsilon_{lz}^{B}(\mathbf{r}_\parallel,z)\big|_{z=0}=\Gamma_{li}[\lambda_{izpq}\varepsilon_{pq}^{(0)}-\lambda_{iz\alpha\beta}\varepsilon_{\alpha\beta}^{B}(\mathbf{r}_\parallel,z)\big|_{z=0}]. \quad \text{(B4)}$$

By substituting $\varepsilon_{lz}^{B}(\mathbf{r}_\parallel,z)\big|_{z=0}$ from Eq. (B4) into Eq. (B1), one obtains the elastic energy in the form where only in-plane components of the strain tensor $\varepsilon_{\alpha\beta}^{B}(\mathbf{r}_\parallel,z)\big|_{z=0}$ enter,

$$E_{\text{elastic}}^{SB}=-h^S\int d^2\mathbf{r}_\parallel\Theta^S(\mathbf{r}_\parallel)[\lambda_{\alpha\beta pq}-\lambda_{\alpha\beta iz}\Gamma_{il}\lambda_{lzpq}]\varepsilon_{pq}^{(0)}\varepsilon_{\alpha\beta}^{B}(\mathbf{r}_\parallel,z)\big|_{z=0}-h^S\int d^2\mathbf{r}_\parallel\Theta^S(\mathbf{r}_\parallel)\varepsilon_{pq}^{(0)}\lambda_{pqiz}\Gamma_{il}\lambda_{lzrs}\varepsilon_{rs}^{(0)}. \quad \text{(B5)}$$

In order to understand the physical meaning of the quantity in square brackets in the integrand on the right-hand side of Eq. (B5), we will do the following procedure.

We consider a uniform flat film, lattice mismatched to the substrate, which is coherently conjugated to the substrate, the stress-free strain in the film being $\varepsilon_{ij}^{(0)}$. Then the strain tensor in the film ε_{ij} is determined by conditions of coherent conjugation in the interface plane,

$$\widetilde{\varepsilon_{\alpha\beta}}=0, \quad \text{(B6a)}$$

and by stress-free boundary conditions at the surface,

$$\widetilde{\sigma_{iz}} = \lambda_{izlz}\widetilde{\varepsilon_{lz}} - \lambda_{izpq}\varepsilon_{pq}^{(0)} = 0. \quad \text{(B6b)}$$

The solution of Eq. (B6b) gives $\widetilde{\varepsilon_{lz}} = \Gamma_{li}\lambda_{izpq}\varepsilon_{pq}^{(0)}$, which allows us to obtain the in-plane components of the stress tensor in the uniform film,

$$\widetilde{\sigma_{\alpha\beta}} = \lambda_{\alpha\beta lz}\widetilde{\varepsilon_{lz}} - \lambda_{\alpha\beta pq}\varepsilon_{pq}^{(0)} = -[\lambda_{\alpha\beta pq} - \lambda_{\alpha\beta lz}\Gamma_{li}\lambda_{izpq}]\varepsilon_{pq}^{(0)}. \quad \text{(B7)}$$

By substituting Eq. (B7) into Eq. (B5), we obtain the energy of the interaction of the array of surface islands and of the array of buried islands as follows:

$$E_{\text{elastic}}^{SB} = h^S \int d^2\mathbf{r}_\parallel \Theta^S(\mathbf{r}_\parallel)\widetilde{\sigma_{\alpha\beta}}\varepsilon_{\alpha\beta}^B(\mathbf{r},z)\big|_{z=0} - h^S \int d^2\mathbf{r}_\parallel \Theta^S(\mathbf{r}_\parallel)\varepsilon_{pq}^{(0)}\lambda_{pqiz}\Gamma_{il}\lambda_{lzrs}\varepsilon_{rs}^{(0)}. \quad \text{(B8)}$$

Here the first term on the right-hand side of Eq. (B8) is obtained is the required form containing only in-plane components of the strain tensor. Since the second term does not contain the strain due to the buried island, it can be omitted from the interaction energy. This gives us the interaction energy in the form of Eq. (2.20).

*Permanent address: A. F. Ioffe Physical Technical Institute, St. Petersburg 194021, Russia. Electronic address: shchukin@sol.physik.TU-Berlin.DE

[1] A. G. Khachaturyan, *Theory of Structural Transformations in Solids* (Wiley, New York, 1983).

[2] V. I. Marchenko, Pis'ma Zh. Eksp. Teor. Fiz. **33**, 397 (1981) [JETP Lett. **33**, 381 (1981)].

[3] O. L. Alerhand, D. Vanderbilt, R. D. Meade, and J. D. Joannopoulos, Phys. Rev. Lett. **61**, 1973 (1988).

[4] I. P. Ipatova, V. G. Malyshkin, and V. A. Shchukin, J. Appl. Phys. **74**, 7198 (1993); Philos. Mag. B **70**, 557 (1994).

[5] V. A. Shchukin, N. N. Ledentsov, P. S. Kop'ev, and D. Bimberg, Phys. Rev. Lett. **75**, 2968 (1995); V. A. Shchukin, N. N. Ledentsov, M. Grundmann, P. S. Kop'ev, and D. Bimberg, Surf. Sci. **352-354**, 117 (1996).

[6] N. N. Ledentsov, M. Grundmann, N. Kirstaedter, O. Schmidt, R. Heitz, J. Böhrer, D. Bimberg, V. M. Ustinov, V. A. Shchukin, P. S. Kop'ev, Zh. I. Alferov, S. S. Ruvimov, A. O. Kosogov, P. Werner, U. Richter, U. Gösele, and J. Heydenreich, Proceedings of the 7th International Conference on Modulated Semiconductor Structures, Madrid, 1995 [Solid-State Electron. **40**, 785 (1996)].

[7] D. E. Jesson, K. M. Chen, and S. J. Pennycook, MRS Bull. **21**, 31 (1996); D. E. Jesson, K. M. Chen, S. J. Pennycook, T. Thundat, and R. J. Warmack, Phys. Rev. Lett. **77**, 1330 (1996).

[8] J. Tersoff, Phys. Rev. Lett. **77**, 2017 (1996).

[9] P. D. Wang, N. N. Ledentsov, C. M. Sotomayor Torres, P. S. Kop'ev, and V. M. Ustinov, Appl. Phys. Lett. **64**, 1526 (1994); **66**, 112 (1995).

[10] V. Bressler-Hill, A. Lorke, S. Yarma, K. Pond, P. M. Petroff, and W. H. Weinberg, Phys. Rev. B **50**, 8479 (1994).

[11] G. M. Guryanov, G. E. Cirlin, A. O. Golubok, S. Ya. Tipisev, N. N. Ledentsov, V. A. Shchukin, M. Grundmann, D. Bimberg, and Zh. I. Alferov, Surf. Sci. **352-354**, 646 (1996).

[12] L. Goldstein, F. Glas, J. Y. Marzin, M. N. Charasse, and G. Le Roux, Appl. Phys. Lett. **47**, 1099 (1985).

[13] S. Guha, A. Madhukar, and K. C. Rajkumar, Appl. Phys. Lett. **57**, 2110 (1990).

[14] D. Leonard, M. Krishnamurthy, C. M. Reaves, S. P. Denbaars, and P. M. Petroff, Appl. Phys. Lett. **63**, 3203 (1993).

[15] J. M. Moison, F. Houzay, F. Barthe, L. Leprince, E. André, and O. Vate, Appl. Phys. Lett. **64**, 196 (1994).

[16] J.-Y. Marzin, J.-M. Gérard, A. Izraël, D. Barrier, and G. Bastard, Phys. Rev. Lett. **73**, 716 (1994).

[17] N. N. Ledentsov, M. Grundmann, N. Kirstaedter, J. Christen, R. Heitz, J. Böhrer, F. Heinrichsdorf, D. Bimberg, S. S. Ruvimov, P. Werner, U. Richter, U. Gösele, J. Heydenreich, V. M. Ustinov, A. Yu. Egorov, M. V. Maximov, P. S. Kop'ev, and Zh. I. Alferov, in *Proceedings of the 22nd International Conference on the Physics of Semiconductors, Vancouver, Canada, 1994*, edited by D. J. Lockwood (World Scientific, Singapore, 1994), Vol. 3, p. 1855.

[18] D. Bimberg, M. Grundmann, N. N. Ledentsov, S. S. Ruvimov, P. Werner, U. Richter, J. Heydenreich, V. M. Ustinov, P. S. Kop'ev, and Zh. I. Alferov, Thin Solid Films **267**, 32 (1995).

[19] M. Grundmann, J. Christen, N. N. Ledentsov, J. Böhrer, D. Bimberg, S. S. Ruvimov, P. Werner, U. Richter, U. Gösele, J. Heydenreich, V. M. Ustinov, A. Yu. Egorov, A. E. Zhukov, P. S. Kop'ev, and Zh. I. Alferov, Phys. Rev. Lett. **74**, 4043 (1995).

[20] M. Grundmann, N. N. Ledentsov, R. Heitz, L. Eckey, J. Christen, J. Böhrer, D. Bimberg, S. S. Ruvimov, P. Werner, U. Richter, U. Gösele, J. Heydenreich, V. M. Ustinov, A. Yu. Egorov, A. E. Zhukov, P. S. Kop'ev, and Zh. I. Alferov, Phys. Status Solidi B **188**, 249 (1995).

[21] M. Grundmann, O. Stier, and D. Bimberg, Phys. Rev. B **52**, 11 969 (1995).

[22] F. Heinrichsdorff, A. Krost, M. Grundmann, D. Bimberg, A. Kosogov, and P. Werner, Appl. Phys. Lett. **68**, 3284 (1996).

[23] T. S. Kuan and S. S. Iyer, Appl. Phys. Lett. **59**, 2242 (1991).

[24] J. Y. Yao, T. G. Andersson, and G. L. Dunlop, J. Appl. Phys. **69**, 2224 (1991).

[25] Q. Xie, P. Chen, and A. Madhukar, Appl. Phys. Lett. **65**, 2051 (1994).

[26] Q. Xie, A. Madhukar, P. Chen, and N. Kobayashi, Phys. Rev. Lett. **75**, 2542 (1995).

[27] G. S. Solomon, J. A. Trezza, A. F. Marshall, and J. S. Harris, Jr., Phys. Rev. Lett. **76**, 952 (1996).

[28] J. Tersoff, C. Teichert, and M. G. Lagally, Phys. Rev. Lett. **76**, 1675 (1996).

[29] N. N. Ledentsov, V. A. Shchukin, M. Grundmann, N. Kirstaedter, J. Böhrer, O. Schmidt, D. Bimberg, V. M. Ustinov, A. Yu. Egorov, A. E. Zhukov, P. S. Kop'ev, S. V. Zaitsev, N. Yu. Gordeev, Zh. I. Alferov, A. I. Borovkov, A. O. Kosogov, S. S. Ruvimov, P. Werner, U. Gösele, and J. Heydenreich, Phys. Rev. B **54**, 8743 (1996).

[30] N. N. Ledentsov, J. Böhrer, D. Bimberg, I. V. Kochnev, M. V. Maximov, P. S. Kop'ev, Zh. I. Alferov, A. O. Kosogov, S. S. Ruvimov, P. Werner, and U. Gösele, Appl. Phys. Lett. **69**, 1095 (1996).

[31] F. Heinrichsdorff, A. Krost, N. Kirstaedter, M.-H. Mao, M. Grundmann, D. Bimberg, A. O. Kosogov, and P. Werner, Jpn. J. Appl. Phys. Part 1 **36**, 1129 (1997).

[32] I. T. Ferguson, A. G. Norman, T. Y. Seong, G. R. Booker, R. H.

Thomas, C. C. Phillips, and R. A. Stradling, Appl. Phys. Lett. **59**, 3324 (1991).
[33] K. Y. Cheng, K.-C. Hsieh, and J. N. Baillargeon, Appl. Phys. Lett. **60**, 2892 (1992).
[34] B. J. Wu, J. M. De Puydt, G. M. Haugen, G. E. Höfler, M. A. Haase, H. Cheng, S. Guha, J. Qin, L. H. Kuo, and L. Salamanca-Riba, Appl. Phys. Lett. **66**, 3462 (1995).
[35] S. W. Jun, T.-Y. Seong, J. H. Lee, and B. Lee, Appl. Phys. Lett. **68**, 3443 (1996).
[36] R. Schur, F. Sogawa, M. Nishioka, S. Ishida, and Y. Arakawa, Jpn. J. Appl. Phys., Part 2 **35**, L857 (1997).
[37] N. N. Ledentsov, D. Bimberg, Yu. M. Shernyakov, V. Kochnev, M. V. Maximov, A. V. Sakharov, I. L. Krestnikov, A. Yu. Egorov, A. F. Tsatsul'nikov, B. V. Volovik, V. M. Ustinov, P. S. Kop'ev, Zh. I. Alferov, A. O. Kosogov, and P. Werner, Appl. Phys. Lett. **70**, 2888 (1997).
[38] N. N. Ledentsov, I. L. Krestnikov, M. V. Maximov, S. V. Ivanov, S. L. Sorokin, P. S. Kop'ev, Zh. I. Alferov, D. Bimberg, and C. M. Sotomayor Torres, Appl. Phys. Lett. **69**, 1343 (1996); **70**, 2766 (1997).
[39] M. Straßburg, V. Kutzer, U. W. Pohl, A. Hoffmann, I. Broser, N. N. Ledentsov, D. Bimberg, A. Rosenauer, U. Fischer, D. Gerthsen, I. L. Krestnikov, M. V. Maximov, P. S. Kop'ev, and Zh. I. Alferov, Appl. Phys. Lett. **72**, 942 (1998).
[40] D. Vanderbilt, Surf. Sci. **268**, L300 (1992).
[41] Kwok-On Ng and D. Vanderbilt, Phys. Rev. B **52**, 2177 (1995).
[42] See, for example, the review by J. D. Eshelby, *Solid State Physics*, edited by F. Seitz and D. Turnbull (Academic, New York, 1956), Vol. 3, p. 79.
[43] A. A. Maradudin and R. F. Wallis, Surf. Sci. **91**, 423 (1980).
[44] K. Portz and A. A. Maradudin, Phys. Rev. B **16**, 3535 (1977).
[45] V. G. Malyshkin, and V. A. Shchukin, Semiconductors **27**, 1062 (1993).
[46] I. P. Ipatova, V. G. Malyshkin, A. A. Maradudin, V. A. Shchukin, and R. F. Wallis, Phys. Rev. B (to be published).
[47] V. I. Marchenko and A. Ya. Parshin, Zh. Eksp. Teor. Fiz. **79**, 257 (1980) [Sov. Phys. JETP **52**, 129 (1980)].
[48] A. Garcia and J. E. Northrup, Phys. Rev. B **48**, 17 350 (1993).
[49] J. Dabrowski, E. Pehlke, and M. Scheffler, Phys. Rev. B **49**, 4790 (1994).
[50] A. Grossmann, W. Erley, J. B. Hannon, and H. Ibach, Phys. Rev. Lett. **77**, 127 (1996).
[51] G. W. Farnell, *Properties of Elastic Surface Waves*, in *Physical Acoustic*, edited by W. P. Mason and R. N. Thurston (Academic, New York, 1970), Vol. 6.
[52] A. M. Kosevich, Yu. A. Kosevich, and E. S. Syrkin, Zh. Eksp. Teor. Fiz. **88**, 1089 (1985) [Sov. Phys. JETP **61**, 639 (1985)].
[53] Semiconductors, *Physics of II-VI and I-VII Compounds, Semimagnetic Semiconductors*, Landolt-Börnstein, Vol. 17b, edited by O. Madelung (Springer, Berlin, 1982).
[54] *Space Group Symmetry*, edited by T. Hahn, International Tables for Crystallography Vol. A (Reidel, Dordrecht, 1983).
[55] A. A. Maradudin, X. Huang, and A. P. Mayer, J. Appl. Phys. **70**, 53 (1991).